Tight Robust Formulation for Uncertain Reserve Activation of an Electric Vehicle Aggregator

Ivan Pavić, Hrvoje Pandžić, Tomislav Capuder
University of Zagreb, Faculty of Electrical Engineering and Computing
Zagreb, Croatia
ivan.pavic@fer.hr, hrvoje.pandzic@fer.hr, tomislav.capuder@fer.hr

***Abstract*—Power system decarbonisation is closely followed by the liberalization of ancillary services to secure a sufficient volume of services at all times. In Europe, system operators are adjusting ancillary services markets to allow entrance of new players. Reserves are the first ones to be liberalized and one of their potential providers are electric vehicles. They can decrease their charging costs through reserve provision under negligible affect on users comfort. However, reserves are highly intertwined with uncertainty and depend on many parameters. To adequately address these uncertainties and safely bid in the markets, an aggregator must adequately integrate them in its optimal bidding algorithm. In this paper, a new robust model is proposed where a tight uncertainty set of reserve activation is created using a realistic reserve activation dataset. The tight robust framework is analysed on the electric vehicle feet operation under one aggregator. A sensitivity analysis is performed to find adequate boundaries of the uncertainty set. The results show that robust approach can be used to adequately address this uncertainty allowing the aggregator to choose its risk exposure and hedging strategy. Also, the results show that neglecting more than 1% of the most extreme activation volumes could lead towards too liberal models not securing the battery limits adequately.**

***Index Terms*—Aggregator, Electric Vehicles, Frequency Containment Reserve, Frequency Restoration Reserve**

I. Introduction

Electric Vehicle (EV) numbers are exponentially growing and they are expected to take up to 30% of the market share worldwide by 2030 [1]. While the EVs' passive charging can harm the power system, smart charging can bring new flexibility and help the system operate more efficiently [2], [3]. In Europe, power system balancing is based on four main types of reserves: Frequency Containment Reserve (FCR), automatic Frequency Restoration Reserve (aFRR), manual Frequency Restoration Reserve (mFRR) and Replacement Reserve (RR). FCR and aFRR are are fast reserves with frequent and short activations, while mFRR and RR are slower with rare and long activations [4]. In this paper only the automatically activated reserves will be addressed as they are technically more suited for battery systems [5] and can bring higher revenues [6].

This work has been supported in part by the European Structural and Investment Funds under project KK.01.2.1.02.0063 SUPER (System for optimization of energy consumption in households)., as well as by the Croatian Science Foundation and European Union through the European Social Fund under project Flexibility of Converter-based Microgrids – FLEXIBASE (PZS-2019-02-7747).

978-1-6654-3597-0/21/$31.00 ©2021 IEEE

Electricity market participants can be affected by different uncertainties stemming from physical or financial conditions. In case of EVs providing reserve, three uncertainty threads can be addressed: EV behavior, prices and reserve activation dynamics. The EV behavior can be modeled using scenarios [7], [8], [9], [10] and solved by second-stage markets [11], [12]. Price uncertainties are often addressed by stochastic [7], [9] or robust frameworks [13]. The last group of uncertainties is often modeled as fixed probability of activation [11], [13], [14] or as stochastic models where scenarios are generated randomly and uniformly [7], [8], [15]. Some more advanced models includes usage of automatic generation control (AGC) signal to design the activation scenarios through a truncated Gaussian distribution [10] or a robust model tackling the worst case scenario of the manual reserve activation [13]. It is worth noting that most of the referenced papers (except [12]) target the United States markets, while European (EU) energy and ancillary service markets are outside of the focus.

The problem of uncertain reserve activation is more prominent then ever before as the structure of reserve providers changed from controllable power plants to distributed resources with constrained possibilities. The EVs' main source of flexibility are their batteries, but at the same time the batteries' state-of-energy (SOE) limits are the most affected parameters when reserve is activated during the real-time. Fixed probabilities or scenarios not based on real activation data do not faithfully represent the uncertainty and the EVs can be forced to dive into unplanned SOE levels, to recharge on other (often more expensive) markets or to be unable to provide the contracted services. The inability to provide the agreed day-ahead (DA) energy would cause additional balancing costs, whereas the inability to deliver the contracted reserve would lead to penalization [10], [14], [15] and potential disqualification. In order to prevent these unwanted events the uncertain nature of reserve activation should be addressed adequately. Activation scenarios based on real data such as Automatic Generation Control – AGC (appropriate for USA markets [10]) or on publicly available balancing data in Europe (ENTSO-e transparency platform) are one of the solutions. However, scenarios can be difficult to create and computationally burdensome. What is more important, such models fail to provide the decision-maker the flexibility in terms of a compromise between the uncertainty and the cost. On the other hand, the robust formulation is not affected by

those issues and as such can be more relevant for this type of problems. A prior work in the area focused on the type of reserves where the number of calls during the day is an integer value accompanied with a binary value for each call meaning that reserve will be either fully activated or not [13]. However, this representation resembles manual reserves and not automatic that are more suitable for EVs.

We argue that there is a scientific gap concerning the modeling of reserve activation uncertainty and thus we propose a new robust framework for EU-style markets based on real balancing data. The focus of the paper is only on reserve activation uncertainty to isolate this concrete issue, but the model can be easily expanded with price or behavior uncertainties explained in the above-referenced papers. The main contribution of the paper is threefold:

1) Reserve activation uncertainty set design based on real activated energy and reserved capacity from EU markets;
2) A new tight robust formulation for the EV fleet automatic reserve bidding;
3) A sensitivity analyses of the robust set parameters affecting the EV fleet and individual EV SOE behavior.

The structure of the paper is the following: Section II defines and explains the mathematical background, Section III identifies the input parameters and elaborates the case studies, while Section IV highlights the most important findings.

II. Mathematical Framework

Two models for an EV fleet optimal scheduling are conceived: the deterministic one and the robust one. The deterministic model stands as the basis for the robust design.

A. Nomenclature

1) Sets and Indices:

$\mathcal{S}$ Set of scenarios, indexed by $s \in [1, N_s]$,
$\mathcal{T}$ Set of time steps, indexed by $t \in [1, N_t]$,
$\mathcal{V}$ Set of vehicles, indexed by $v \in [1, N_v]$.

2) Input Parameters:

Δ Duration of a time-step [h],
Λ Full duration of reserve activation,
$A^{\{\text{UP/DN}\}\_\{\text{FCR/aFRR}\}}$ Fixed Up/Dn FCR/aFRR activation ratio,
C_v^{B} Capital battery cost of vehicle v [€],
$C_{v,t}^{\text{FCH}}$ Fast charging fee [€/kWh],
C_t^{DAM} DA market electricity price at t [€/kWh],
B_v Battery capacity of vehicle v [kWh],
$CA_t^{\{\text{UP/DN}\}\_\{\text{FCR/aFRR}\}}$ Activation fee at t [€/kWh],
$CR_t^{\{\text{UP/DN}\}\_\{\text{FCR/aFRR}\}}$ Reservation fee at t [€/kW/Δ],
$D_{\{1/2/3/4\}}^{\text{B}}$ Battery degradation coefficients,
$E_{v,t}^{\text{RUN}}$ Energy used for driving in vehicle v at t [kWh],
$P_{v,t}^{\text{CP\_MAX}}$ Maximum power limit for ch. stations v at t [kW],
$P^{\text{FCH\_MAX}}$ Maximum power limit for fast charging [kW],
$P_v^{\text{OBC\_MAX}}$ Maximum power limit for OBC of v [kW],
$SOE_v^{\{\text{MIN/MAX}\}}$ Min/max allowed SOE of vehicle v [%],
SOE_v^{T0} Initial SOE of vehicle v [%],
$\eta^{\{\text{SCH/FCH}\}}$ EV slow/fast charging efficiency.
$\eta^{\{\text{RUN/DCH}\}}$ EV mobility/V2G discharging efficiency,

3) Variables:

$c_{v,t}^{\text{DEG}}$ Degradation cost of vehicle v at time t [€],
$e_{v,t}^{\{\text{BUY/SELL}\}\_\text{DAM}}$ Energy bought/sold in DA market [kWh],
$e_{v,t}^{\text{DCH}}$ Energy discharged from vehicle v at t [kWh],
$e_{v,t}^{\{\text{SCH/FCH}\}}$ Energy slow/fast charged to EV v at time t [kWh],
$e_{v,t}^{\text{DEG}}$ Energy flow in/out battery used for degradation,
f Sum of costs other than reserve activation [€],
g Sum of costs of reserve activation [€],
$h_{v,t}$ Energy flow not from reserve activation [MWh],
$k_{v,t}$ Energy flow from reserve activation [MWh],
$r_{v,t}^{\{\text{UP/DN}\}\_\{\text{FCR/aFRR}\}}$ Sold reserve capacity of EV v at t [kW],
$soe_{v,t}^{\text{EV}}$ State-of-energy of EV v at time t [kWh].

B. Deterministic Model

The deterministic model takes a fixed activation ratio based on average activation of specific reserve type and direction [16]. The objective function (OF) includes costs/revenues from the energy market, revenues from the reserve capacity, the V2G degradation cost, the fast charging cost and the costs/revenues of activated reserve energy. The first four costs are summed in eq. (D-2), while the costs associated with reserve activation are summed in eq. (D-3). Objective function:

$$\min_{\Xi_{\mathcal{O}}} \quad (f+g); \tag{D-1}$$

$$\begin{aligned} f = \sum_{t=1}^{N_t} \Big\{ \sum_{v=1}^{N_v} \big[& e_{v,t}^{\text{BUY\_DAM}} \cdot C_t^{\text{DAM}} - e_{v,t}^{\text{SELL\_DAM}} \cdot C_t^{\text{DAM}} \\ & - r_{v,t}^{\text{UP\_FCR}} \cdot CR_t^{\text{UP\_FCR}} - r_{v,t}^{\text{DN\_FCR}} \cdot CR_t^{\text{DN\_FCR}} \\ & - r_{v,t}^{\text{UP\_aFRR}} \cdot CR_t^{\text{UP\_aFRR}} - r_{v,t}^{\text{DN\_aFRR}} \cdot CR_t^{\text{DN\_aFRR}} \\ & + c_{v,t}^{\text{DEG}} + e_{v,t}^{\text{FCH}} \cdot C_{v,t}^{\text{FCH}} \big] \Big\}; \end{aligned} \tag{D-2}$$

$$\begin{aligned} g = \sum_{t=1}^{N_t} \Big\{ \sum_{v=1}^{N_v} \big[& - r_{v,t}^{\text{UP\_FCR}} \cdot A^{\text{UP\_FCR}} \cdot \Delta \cdot CA_t^{\text{UP\_FCR}} \\ & + r_{v,t}^{\text{DN\_FCR}} \cdot A^{\text{DN\_FCR}} \cdot \Delta \cdot CA_t^{\text{DN\_FCR}} \\ & - r_{v,t}^{\text{UP\_aFRR}} \cdot A^{\text{UP\_aFRR}} \cdot \Delta \cdot CA_t^{\text{UP\_aFRR}} \\ & + r_{v,t}^{\text{DN\_aFRR}} \cdot A^{\text{DN\_aFRR}} \cdot \Delta \cdot CA_t^{\text{DN\_aFRR}} \big] \Big\}; \end{aligned} \tag{D-3}$$

Eq. (D-2) manages the costs not associated with reserve activation, while the costs stemming from the reserve activation are summed in eq. (D-3). Such division of OF is used to ease the writing and understanding of the equations in Section II-C.

$$\begin{aligned} & e_{v,t}^{\text{BUY\_DAM}}, e_{v,t}^{\text{SELL\_DAM}}, r_{v,t}^{\text{UP\_FCR}}, \\ & r_{v,t}^{\text{DN\_FCR}}, r_{v,t}^{\text{UP\_aFRR}}, r_{v,t}^{\text{DN\_aFRR}} \geq 0; \end{aligned} \tag{D-4}$$

$$\begin{aligned} & e_{v,t}^{\text{SELL\_DAM}}/\Delta - e_{v,t}^{\text{BUY\_DAM}}/\Delta + r_{v,t}^{\text{UP\_FCR}} + r_{v,t}^{\text{UP\_aFRR}} \\ & \leq min(P_v^{\text{OBC\_MAX}}, P_{v,t}^{\text{CP\_MAX}}); \end{aligned} \tag{D-5}$$

$$\begin{aligned} & e_{v,t}^{\text{BUY\_DAM}}/\Delta - e_{v,t}^{\text{SELL\_DAM}}/\Delta + r_{v,t}^{\text{DN\_FCR}} + r_{v,t}^{\text{DN\_aFRR}} \\ & \leq min(P_v^{\text{OBC\_MAX}}, P_{v,t}^{\text{CP\_MAX}}); \end{aligned} \tag{D-6}$$

The DA variables are modeled as positive values in eq. (D-4). Charging/discharging power is limited with the On-Board Charger (OBC) and Charging Point capacity in eqs. (D-5) and (D-6). The lower value limits the exchanged power with grid.

$$soe_{v,t}^{\text{EV}} = SOE^{\text{T0}} \cdot B_v + h_{v,t} + k_{v,t}; \tag{D-7}$$

$$h_{v,t} = \sum_{\tau=1}^{t} \{ e_{v,\tau}^{\text{BUY\_DAM}} \cdot \eta^{\text{CH}} - e_{v,\tau}^{\text{SELL\_DAM}}/\eta^{\text{DCH}}$$

$$-E^{\text{RUN}}_{v,\tau}/\eta^{\text{RUN}} + e^{\text{FCH}}_{v,\tau} \cdot \eta^{\text{FCH}}\}; \quad \text{(D-8)}$$

$$k_{v,t} = \sum\nolimits_{\tau=1}^{t} \{\Delta \cdot [\eta^{\text{CH}} \cdot (r^{\text{DN\_FCR}}_{v,\tau} \cdot A^{\text{DN\_FCR}} + r^{\text{DN\_aFRR}}_{v,\tau} \cdot A^{\text{DN\_aFRR}}) - 1/\eta^{\text{DCH}} \cdot (r^{\text{UP\_FCR}}_{v,\tau} \cdot A^{\text{UP\_FCR}} + r^{\text{UP\_aFRR}}_{v,\tau} \cdot A^{\text{UP\_aFRR}})]\}; \quad \text{(D-9)}$$

The SOE is calculated as a summation of the initial SOE and all the energy charged/discharged to/from the battery until the time-step t in eq. (D-7). Similarly as in the OF equation (D-1), the eq. (D-7) has its terms divided into two categories: variable $h_{v,t}$ defined in eq. (D-8) deals with variables not associated with reserve activation, while the variable $k_{v,t}$ defined in eq. (D-9) deals with reserve activation variables (later modeled as random parameters). Energy charged/discharged as reserve activation is calculated with inputs $A^{\{\text{UP/DN}\}\_\{\text{FCR/aFRR}\}} \in [0, 1]$. Note that in det. case these are fixed scalars, however in subsequent Section, they will be changed to random parameters.

$$SOE^{\text{MIN}} \cdot B_v \leq soe^{\text{EV}}_{v,t} + e^{\text{BUY\_DAM}}_{v,t+1} \cdot \eta^{\text{CH}} - e^{\text{SELL\_DAM}}_{v,t+1}/\eta^{\text{DCH}} - \Lambda \cdot \Delta/\eta^{\text{DCH}} \cdot (r^{\text{UP\_FCR}}_{v,t+1} + r^{\text{UP\_aFRR}}_{v,t+1}) - E^{\text{RUN}}_{v,t+1}/\eta^{\text{RUN}} + e^{\text{FCH}}_{v,t+1} \cdot \eta^{\text{FCH}} \quad \forall t \in \mathcal{T}_{(t \neq Nt)}; \quad \text{(D-10)}$$

$$SOE^{\text{MAX}} \cdot B_v \geq soe^{\text{EV}}_{v,t} + e^{\text{BUY\_DAM}}_{v,t+1} \cdot \eta^{\text{CH}} - e^{\text{SELL\_DAM}}_{v,t+1}/\eta^{\text{DCH}} + \Lambda \cdot \Delta \cdot \eta^{\text{CH}} \cdot (r^{\text{DN\_FCR}}_{v,t+1} + r^{\text{DN\_aFRR}}_{v,t+1}) - E^{\text{RUN}}_{v,t+1}/\eta^{\text{RUN}} + e^{\text{FCH}}_{v,t+1} \cdot \eta^{\text{FCH}} \quad \forall t \in \mathcal{T}_{(t \neq Nt)}; \quad \text{(D-11)}$$

$$SOE^{\text{T0}} \cdot B_v \leq soe^{\text{EV}}_{v,t} \leq SOE^{\text{MAX}} \cdot B_v \text{ for } t = N_t; \quad \text{(D-12)}$$

$$0 \leq e^{\text{FCH}}_{v,t} \leq P^{\text{FCH\_MAX}} \cdot \Delta; \quad \text{(D-13)}$$

Battery capacity is limited with eqs. (D-10) and (D-11) considering the full activation of the reserves. Those two equations ensure that the SOE will be sufficient in the worst case of the reserve activation. The SOE in the final timestep is constrained with Eq. (D-12), while the fast charging limit is set in (D-13). V2G degradation calculus used in this paper is used as in [17]. Eqs (D-4)–(D-13) are valid $\forall v \in \mathcal{V}$ and $\forall t \in \mathcal{T}$, except for eqs. (D-10) – (D-11) which don't apply the final timestep, and (D-12), which applies only in the last step.

C. Robust Model

Compared to the deterministic model, the activation ratios in robust model are uncertain parameters ($a^{\{\text{UP/DN}\}\_\{\text{FCR/aFRR}\}}_{v,\tau,t}$) bounded by the uncertainty set (US) under eqs. (US-1)–(US-15). OF minimizes the total cost (R-1) and maximizes the reserve activation (mimicking the worst-case realization) using eqs. (R-4)–(R-8). Objective function:

$$\min_{\Xi_{\mathcal{O}}} \quad (z) \quad \text{(R-1)}$$

subject to:

$$\text{(D-2)}, \text{(D-4)} - \text{(D-6)}, \text{(D-8)}, \text{(D-13)} \; ; \quad \text{(R-2)}$$

$$\text{(D-3)}, \text{(D-9)}; \quad \text{(R-3)}$$

$$\max_{\Xi_{\mathcal{A}}} \; (g^{\text{RA}}) \leq z - g^{\text{NRA}}; \quad \text{(R-4)}$$

$$\max_{\Xi_{\mathcal{A}}}(-h^{\text{RA}}_{v,t}) \leq B_v \cdot (SOE^{\text{T0}} - SOE^{\text{MIN}}) \quad \text{(R-5)}$$
$$-\Lambda \cdot \Delta/\eta^{\text{DCH}} \cdot (r^{\text{UP\_FCR}}_{v,t+1} + r^{\text{UP\_aFRR}}_{v,t+1}) + h^{\text{NRA}}_{v,t+1};$$

$$\max_{\Xi_{\mathcal{A}}}(h^{\text{RA}}_{v,t}) \leq B_v \cdot (SOE^{\text{MAX}} - SOE^{\text{T0}}) \quad \text{(R-6)}$$
$$-\Lambda \cdot \Delta \cdot \eta^{\text{CH}} \cdot (r^{\text{DN\_FCR}}_{v,t+1} + r^{\text{DN\_aFRR}}_{v,t+1}) - h^{\text{NRA}}_{v,t+1};$$

$$\max_{\Xi_{\mathcal{A}}} \; (h^{\text{RA}}_{v,t}) \leq B_v \cdot (SOE^{\text{MAX}} - SOE^{\text{T0}}) - h^{\text{NRA}}_{v,t}; \quad \text{(R-7)}$$

$$\max_{\Xi_{\mathcal{A}}} \; (-h^{\text{RA}}_{v,t}) \leq h^{\text{NRA}}_{v,t}, \quad \text{for} \quad t = N_t; \quad \text{(R-8)}$$

To be able to solve the master problem with four related maximization subproblems, the model is reformulated using the methodology presented in [18]. Eqs. (R-2) are taken unaltered from the det. model, while eqs. (R-3) uses an activation variable instead of a fixed activation parameter. Each of the constraints (including OF) with uncertain parameters from (R-3) are modeled as independent maximization subproblems (R-4)–(R-8). OF of the deterministic model eq. (D-1) is recast as a robust subproblem in eqs. (R-1) and (R-4). SOE bounds from Eqs. (D-10)–(D-12) are reformulated in eqs. (R-5)–(R-8).

D. Uncertainty Set

The US is necessary to bound the uncertain reserve activation parameters which are recast as variables of the inner subproblems (R-5)–(R-8). The US stems from the real data taken from RTE for 2018, where the activation ratio is calculated as *FCR/aFRR Activated Reserve Energy* divided by (*FCR/aFRR Accepted Reserve Capacity* $\cdot\Delta$) in each half-hourly timestep.

After a detailed statistical evaluation for each reserve type (statistics for FCR are shown in Figures 1a–1b, due to succinctness of the paper the aFRR analysis is omitted) two main sets of constraints were constructed: one for single activation in each timestep shown in Figure 1a and one for daily summation of activations shown in Figure 1b. Within each of these sets, three uncertain parameters are observed: up (the top graph on each subfigure), down (the right graph) and up+down activation (the bottom graph). On each of these graphs three areas are defined, the distribution between the borders: min and max (Q0 – yellow), 1% and 99% (Q1 – green) and 5% and 95% (Q5 – red) of the uncertain parameter.

Each of those areas represent a tested scenario for sensitivity analysis (apart those, two more scenarios are tested: Q10 and Q25, but these are omitted from figures as too many borders make figures hard to read and understand). On scatter graph in the center of the subfigures we can see an interrelation between the up and down uncertain parameters where the borders from all three side graphs are displayed (vertical lines – up, horizontal lines – down, slope lines – up + down activation border). The shaded areas in the scatter graph represent the area of a specific budget of uncertainty between all borders (yellow, green, red).

For example, if the Figure 1a is to be observed the upper left graph represents the distribution of the FCR up reserve activation ratios in half-hour resolution. It can be seen that 95% of activations is less than 21% (red curve) of the total available FCR up capacity. On the same graph, it could be seen that the half-hourly activations never cross the 47% (yellow curve) of the total available capacity. In the same manner the leftmost graph displays the down FCR data, and

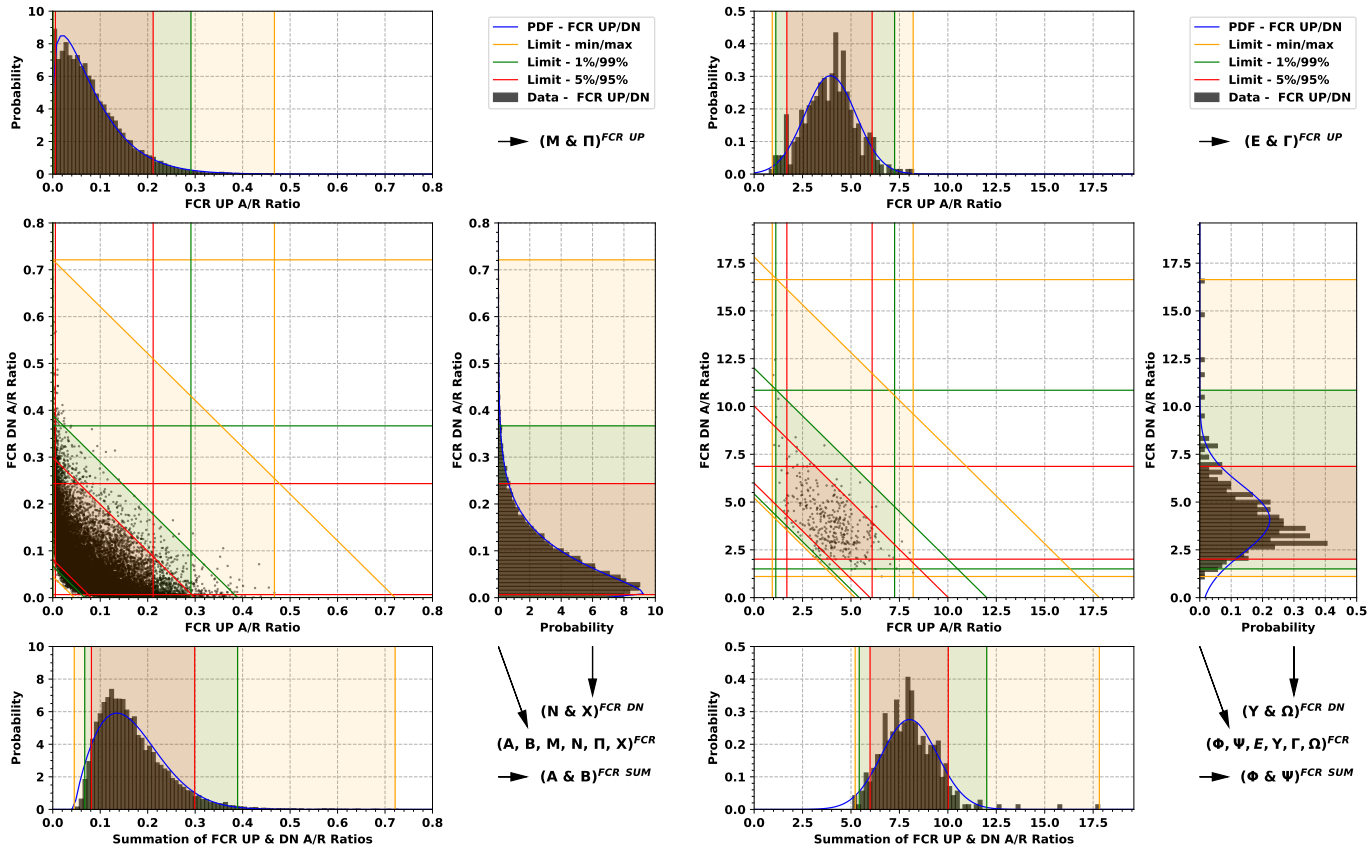

(a) FCR Activation/Reservation Ratios

(b) Daily Summations of FCR Activation/Reservation Ratios

Fig. 1: Statistical Plots of FCR Activation/Reservation Ratios

the lowest graph displays the summation of up and down FCR activation ratios. The middle scatter graph provides the mutual dependence of up and down FCR activations. The yellow slope line, from 0.72 down ratio to 0.72 up ratio, presents the limit for the summation of the up and down ratios (i.e. half hourly sumations of ratios never pass the 72% of total capacity), whereas the green slope line from 0.38-0.38 presents the limit which the summation of up and down FCR ratios crossed only 1% of all half-hourly timesteps.

The graphically presented constraints from the Figure 1 are mathematically represented with the following US equations: $\forall\ (a^{\text{UP\_FCR}}_{v,\tau,t}, a^{\text{DN\_FCR}}_{v,\tau,t}, a^{\text{UP\_aFRR}}_{v,\tau,t}, a^{\text{DN\_aFRR}}_{v,\tau,t}) \in \mathcal{A}$, where $\mathcal{A}$ is:

$$\mathcal{A} = \{a^{\text{UP\_FCR}}_{v,\tau,t}, a^{\text{DN\_FCR}}_{v,\tau,t}, a^{\text{UP\_aFRR}}_{v,\tau,t}, a^{\text{DN\_aFRR}}_{v,\tau,t} \quad |$$

$$a^{\text{UP\_FCR}}_{v,\tau,t}, a^{\text{DN\_FCR}}_{v,\tau,t}, a^{\text{UP\_aFRR}}_{v,\tau,t}, a^{\text{DN\_aFRR}}_{v,\tau,t} \geq 0; \quad \text{(US-1)}$$

$$a^{\text{UP\_FCR}}_{v,\tau,t} + a^{\text{DN\_FCR}}_{v,\tau,t} \geq A^{\text{FCR}} : \alpha^{\text{(R-5)\_FCR}}_{v,\tau,t}; \quad \text{(US-2)}$$

$$a^{\text{UP\_FCR}}_{v,\tau,t} + a^{\text{DN\_FCR}}_{v,\tau,t} \leq B^{\text{FCR}} : \beta^{\text{(R-5)\_FCR}}_{v,\tau,t}; \quad \text{(US-3)}$$

$$a^{\text{UP\_FCR}}_{v,\tau,t} \geq \Pi^{\text{FCR}} : \pi^{\text{(R-5)\_FCR}}_{v,\tau,t}; \quad \text{(US-4)}$$

$$a^{\text{DN\_FCR}}_{v,\tau,t} \geq X^{\text{FCR}} : \chi^{\text{(R-5)\_FCR}}_{v,\tau,t}; \quad \text{(US-5)}$$

$$a^{\text{UP\_FCR}}_{v,\tau,t} \leq M^{\text{FCR}} : \mu^{\text{(R-5)\_FCR}}_{v,\tau,t}; \quad \text{(US-6)}$$

$$a^{\text{DN\_FCR}}_{v,\tau,t} \leq N^{\text{FCR}} : \nu^{\text{(R-5)\_FCR}}_{v,\tau,t}; \quad \text{(US-7)}$$

$$\sum\nolimits_{\tau=1}^{t} a^{\text{UP\_FCR}}_{v,\tau,t} + \sum\nolimits_{\tau=1}^{t} a^{\text{DN\_FCR}}_{v,\tau,t} \geq \Phi^{\text{FCR}}_{t} : \phi^{\text{(R-5)\_FCR}}_{v,t}; \quad \text{(US-8)}$$

$$\sum\nolimits_{\tau=1}^{t} a^{\text{UP\_FCR}}_{v,\tau,t} + \sum\nolimits_{\tau=1}^{t} a^{\text{DN\_FCR}}_{v,\tau,t} \leq \Psi^{\text{FCR}}_{t} : \psi^{\text{(R-5)\_FCR}}_{v,t}; \quad \text{(US-9)}$$

$$\sum\nolimits_{\tau=1}^{t} a^{\text{UP\_FCR}}_{v,\tau,t} \geq E^{\text{FCR}}_{t} : \epsilon^{\text{(R-5)\_FCR}}_{v,t}; \quad \text{(US-10)}$$

$$\sum\nolimits_{\tau=1}^{t} a^{\text{DN\_FCR}}_{v,\tau,t} \geq \Upsilon^{\text{FCR}}_{t} : \upsilon^{\text{(R-5)\_FCR}}_{v,t}; \quad \text{(US-11)}$$

$$\sum\nolimits_{\tau=1}^{t} a^{\text{UP\_FCR}}_{v,\tau,t} \leq \Gamma^{\text{FCR}}_{t} : \gamma^{\text{(R-5)\_FCR}}_{v,t}; \quad \text{(US-12)}$$

$$\sum\nolimits_{\tau=1}^{t} a^{\text{DN\_FCR}}_{v,\tau,t} \leq \Omega^{\text{FCR}}_{t} : \omega^{\text{(R-5)\_FCR}}_{v,t}; \quad \text{(US-13)}$$

(US-2) - (US-13) are analogous for aFRR; (US-14)

(US-2) - (US-14) are similar for (R-4) - (R-8).$\}$ (US-15)

The borders are modeled using the US under eqs. (US-1) - (US-13) for the *FCR* service and for the subproblem stated in (R-5). The (US-14) spreads it over *aFRR* service and (US-15) over other robust subproblems. For constraints (R-5) and (R-6) the US is applied up to a specific time-step t and for a specific EV v. The US equations, uncertain parameters and dual variables for (R-6) are the same as for (R-5). For subproblems (R-4), (R-7) and (R-8) equations are similar in nature but have different indices: US for OF (R-4) is applied over the whole observed horizon $[1, N_t]$ and over the whole observed fleet $[1, N_v]$, whereas for the (R-8) it is applied up to the last time-step Nt and for specific EV v.

The connection of the graphical and mathematical US constraints is indicated in Figure 1 on top and bottom right

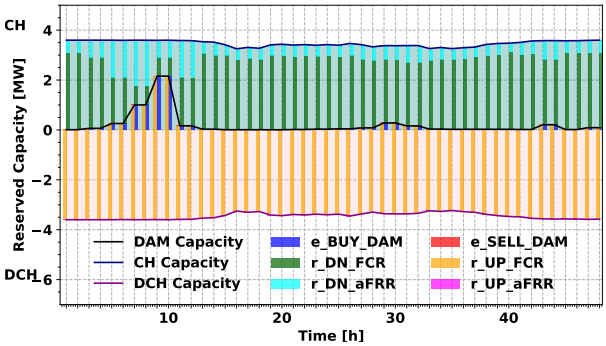

Fig. 2: Deterministic Case Scheduling Results

corners of each subfigure, e.g. on Subfigure 1a limits for eqs. (US-4) and (US-6) are stated in the top right corner. Note that the upper case Greek letters on Figure 1 are the right hand sides of the US equations.

III. Testing and Validation

To validate the goal of the robust model and to enable EV reserve provision without exceeding the SOE limits, the deterministic model with average yearly activation ratios will serve as a reference case. The robust model will be tested with 5 different USs, each representing a quantile of the observed random parameter: 0 (Q0), 1 (Q1), 5 (Q5), 10 (Q10), 25% (Q25). For example, US of 5% for the UP FCR activation ratio means neglecting the 5% of the lowest (Π^{FCR}) and highest (M^{FCR}) values of the UP FCR activation (red curves/area in the top graph in Figure 1a).

A. Input Parameters

The EV driving/parking behaviour from the JRC European driving study [19] and [20] was used and reformulated as two input parameters used in this paper: EV driving consumption ($E^{\text{RUN}}_{v,t}$ in eq. (D-7)) and maximum possible CP energy ($E^{\text{CP\_MAX}}_{v,t}$ in eqs. (D-5) and (D-6)). The EV behaviour for France was simulated with total number of EVs 581. Vehicle type and trip data was used as the basis to create three EV models for this simulations with three distinct parameters: battery capacity, OBC size, and fleet share. Those three types are: small EV (20 kWh, 3.7 kW, 30%), medium EV (40 kWh, 7.4 kW, 40%) and large EV (60 kWh, 11 kW, 30%). In total, the fleet's battery capacity is 23 MWh, whereas the installed OBC power is 4 MW. For the simulation purposes, the price data (energy and reserve) is also used for the French power system. From the French EPEX DA market price (September 21, 2018 – average: 48.86 €/MWh) and from the RTE website the FCR reserve price (first week of 2019 – 4.83 €/MW/0.5h) are taken. Since aFRR during that period was priced at a regulated fee, that fee is used for both directions: 4.84 €/MW/0.5h.

B. Results

The scheduling results are shown in Figures 2–3, whereas the ex-post simulation results using 100 real-world scenarios are summarized in Figure 4. Figures 2–3 show the solution of DA bidding variables in MW over whole fleet in each timestep.

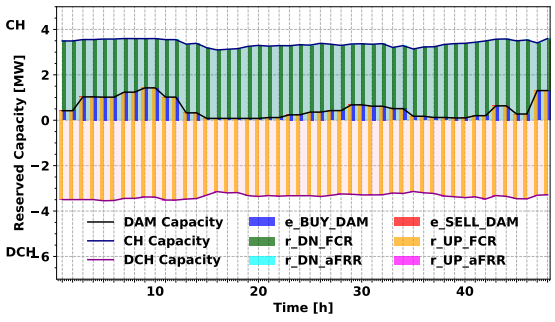

(a) Robust Case – US: Q25

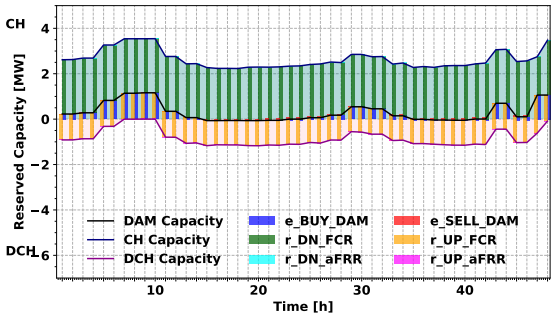

(b) Robust Case – US: Q5

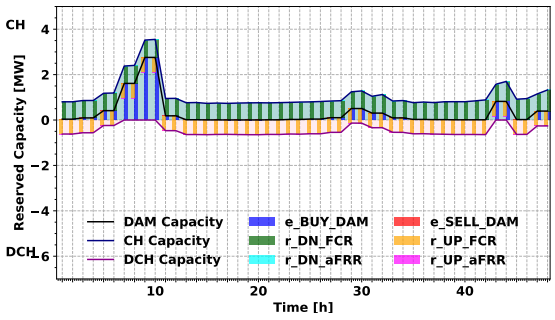

(c) Robust Case – US: Q0

Fig. 3: Robust Cases Scheduling Results

Figure 4 shows four types of model validation parameters: min/max ind. SOE (right axis in %) and min/max fleet-wise energy exceeding the SOE limits (left axis in MWh). All validation parameters refer to the worst-case scenario. Figure 2 shows the DA plans for the reference deterministic case, whereas Figure 3 show the robust model results for the US of 25, 5, and 0% quantiles. The deterministic case bids in the reserve market in a very wide range where average bid reserve capacites are 6.29 and 4.49 fleet-wise for up and down FCR, respectively (Figure 2). The mild activation constraints of 25% quantile do not consider more than 50% of realized historic activations and such bidding is even more intense where average bid capacities are 6.67 and 4.95 MW for up and down FCR, respectively (Figures 3a). Tightening the activation constraints to 5% quantile, to be closer to their min/max values, the amount of bid capacities decreases and in average it makes 1.94 and 4.05 MW for up and down FCR, respectively (Figure 3b). The smallest amounts of bid capacities are achieved for the tightest constraints set on their min/max values (Figure 3c). In average, for Q0, bid

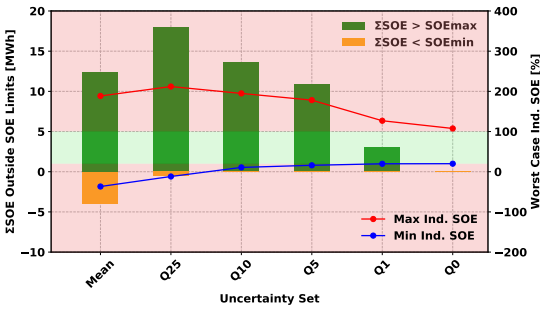

Fig. 4: Comparison of Validation Parameters for Tested Cases

up and down FCR capacities are 1.11 and 1.34, respectively. Note that only deterministic case utilized smaller amounts or aFRR reserve, whereas robust model completely neglected that option. The main reason for such happening is that aFRR is highly more uncertain than FCR.

In correlation to the amount of bid capacities for robust cases, the validation parameters also decrease as the constraints tighten, as shown on Figure 4. It is clear that US of Q25 doesn't sufficiently bound the reserve activation, and that it results in worse solution than deterministic case. The total energy beyond the SOE limits (green + yellow from Figure 4) in Q25 is 18.57 MWh and in deterministic case it is 16.38 MWh. Maximal individual SOE is worse in Q25 than in deterministic case, but the min SOE is better in Q25. Other robust cases have no problems with min SOE constraint at all. Q10 and Q5 have both less fleet-wise energy beyond SOE limits (in total) and slightly better max SOE than det. case but still their results yield too much SOE violations. Q1, however, shows the true face of robust solution where the SOE limits are only slightly violated in over SOE^{MAX} direction with energy exceeding SOE^{MAX} in amount of around 3 MWh with maximal SOE of 126.86%. The Q0 case provides the most conservative solution without any SOE violation whatsoever. In sense of SOE violation this is the best solution, but being conservative in SOE limits aspect directly means lower revenues in financial aspect.

IV. Discussion and Conclusion

This paper proposed a detail robust EV scheduling model which encompasses uncertainty of reserve activation. To create uncertainty sets and validation scenarios real balancing data from European TSOs was used. The statistical analysis of the activation/reservation defined the uncertainty sets. Then the sensitivity analysis on different uncertainty sets (0-25%) was performed and all of them were compared to det. case often used in the literature. The main finding of the paper is the proof that uncertainty of reserve activation can be adequately cast in a robust form and that such models can guarantee EV reserve scheduling without possibility of crossing the SOE limits. Neglecting more than 1% of historic activation can result in too liberal model which doesn't fulfill its task of securing the battery limits. However, models with less than 1% of historic activation are pretty conservative and yield lower profits. The compromise between the covered uncertainty and expected profit must be made while considering the tightness of the robust formulation. The beauty of the proposed model lies in the possibility to use the formulation for other technologies (stationary batteries, power plants...), jointly with other markets and along with other uncertainties such as price, EV behaviour, bidding acceptance etc.

References

[1] International Energy Agency, "Global EV Outlook 2019," 2019.

[2] IRENA (2019), Innovation landscape brief: Electric-vehicle smart charging, International Renewable Energy Agency, Abu Dhabi.

[3] I. Pavić, T. Capuder, and I. Kuzle, "Low carbon technologies as providers of operational flexibility in future power systems," Appl. Energy, vol. 168, pp. 724–738, Apr. 2016.

[4] ENTSO-E, "ENTSO-E Balancing Report," 2020.

[5] Ramboll, "Ancillary Services From New Technologies," 2019.

[6] J. Engels, "Integration of Flexibility from Battery Storage in the Electricity Market," 2020.

[7] M. Alipour, B. Mohammadi-Ivatloo, M. Moradi-Dalvand, and K. Zare, "Stochastic scheduling of aggregators of plug-in electric vehicles for participation in energy and ancillary service markets," Energy, vol. 118, pp. 1168–1179, Jan. 2017.

[8] M. Shafie-Khah, M. P. Moghaddam, M. K. Sheikh-El-Eslami, and J. P. S. Catalão, "Optimised performance of a plug-in electric vehicle aggregator in energy and reserve markets," Energy Convers. Manag., vol. 97, pp. 393–408, Jun. 2015.

[9] I. Momber, A. Siddiqui, T. G. S. Roman, and L. Soder, "Risk averse scheduling by a PEV aggregator under uncertainty," IEEE Trans. Power Syst., vol. 30, no. 2, pp. 882–891, Mar. 2015.

[10] S. I. Vagropoulos and A. G. Bakirtzis, "Optimal bidding strategy for electric vehicle aggregators in electricity markets," IEEE Trans. Power Syst., vol. 28, no. 4, pp. 4031–4041, 2013.

[11] P. Sanchez-Martin, S. Lumbreras, and A. Alberdi-Alen, "Stochastic programming applied to ev charging points for energy and reserve service markets," IEEE Trans. Power Syst., vol. 31, no. 1, Jan. 2016.

[12] C. Goebel and H. A. Jacobsen, "Aggregator-Controlled EV Charging in Pay-as-Bid Reserve Markets with Strict Delivery Constraints," IEEE Trans. Power Syst., vol. 31, no. 6, pp. 4447–4461, Nov. 2016.

[13] M. Kazemi, H. Zareipour, N. Amjady, W. D. Rosehart, and M. Ehsan, "Operation Scheduling of Battery Storage Systems in Joint Energy and Ancillary Services Markets," ITSG, vol. 8, no. 4, Oct. 2017.

[14] M. R. Sarker, Y. Dvorkin, and M. A. Ortega-Vazquez, "Optimal participation of an electric vehicle aggregator in day-ahead energy and reserve markets," IEEE Trans. Power Syst., vol. 31, no. 5, Sep. 2016.

[15] B. Han, S. Lu, F. Xue, and L. Jiang, "Day-ahead electric vehicle aggregator bidding strategy using stochastic programming in an uncertain reserve market," IET Gener. Transm. Distrib., vol. 13, no. 12, Jun. 2019.

[16] I. Pavić, H. Pandžić, T. Capuder, "Electric Vehicles as Frequency Containment Reserve Providers," IEEE International Energy Conference (ENERGYCON), Gammarth, Tunisia, 2020.

[17] I. Pavić, H. Pandžić, and T. Capuder, "Electric vehicle based smart e-mobility system – Definition and comparison to the existing concept," Appl. Energy, vol. 272, p. 115153, Aug. 2020.

[18] J. M. Morales, A. J. Conejo, H. Madsen, P. Pinson, and M. Zugno, Integrating Renewables in Electricity Markets, vol. 205. Boston, MA: Springer US, 2014.

[19] G. Pasaoglu, D. Fiorello, A. Martino, G. Scarcella, A. Alemanno, A. Zubaryeva, C. Thiel, and L. P. O. of the E. Union, "Driving and parking patterns of European car drivers - a mobility survey" 2012.

[20] G. Pasaoglu, D. Fiorello, L. Zani, A. Martino, A. Zubaryeva, and C. Thiel, "Projections for Electric Vehicle Load Profiles in Europe Based on Travel Survey Data Contact information", vol. 1. 2013.